CRYSTAL GROWTH & DESIGN

Article

pubs.acs.org/crystal

Polymorphism and Modulation of Para-Substituted L-Phenylalanine

Leyla-Cann Sögütoglu,[†] Martin Lutz,[‡] Hugo Meekes,[†] René de Gelder,*[,†] and Elias Vlieg[†]

[†]Radboud University, Institute for Molecules and Materials, Heyendaalseweg 135, 6525 AJ, Nijmegen, The Netherlands

[‡]Crystal and Structural Chemistry, Bijvoet Center for Biomolecular Research, Faculty of Science, Utrecht University, Padualaan 8, 3584 CH, Utrecht, The Netherlands

ABSTRACT: The crystal structure of *para*-methyl-L-phenylalanine at 230 K resembles that of the para-fluorinated analogue from the literature but is commensurately modulated with seven molecules in the asymmetric unit ($Z' = 7$). At 100 K, the superstructure loses its modulation, leading to a unit cell with $Z' = 1$, with clear disorder in the phenyl ring orientations. The methyl-substituent in *para*-methyl-L-phenylalanine has, in contrast to fluorine, no polar interactions with protons of neighboring molecules, which might allow for the well-defined modulation of the crystal structure at 230 K.

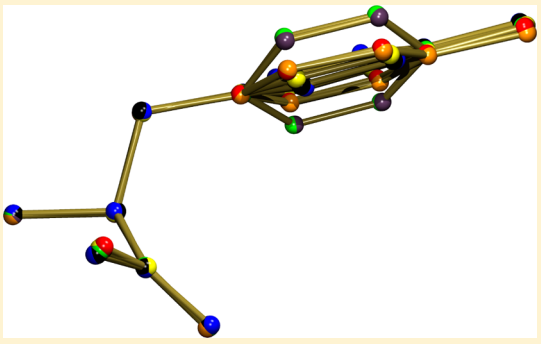

INTRODUCTION

During the past decade, L-phenylalanine (L-Phe) has been studied extensively in its solid state, especially in the framework of being a potential key to understanding the behavior of a large class of important aromatic compounds and peptide-like systems.[1,2] The unique phenyl−phenyl interactions in crystals of this zwitterionic amino acid give rise to a variety of subtle polymorphic forms. The solid state of L-Phe is therefore an elegant model for understanding the simultaneous interplay of weak hydrophobic interactions and strong polar interactions found in amphiphilic systems. Apart from its structural properties, L-Phe has recently gained a significant biochemical interest as well for its possible link to self-assembly in amyloid type systems.[3]

The amphiphilic molecule L-Phe forms layered crystal structures as shown in Figure 1a, consisting of bilayers that stack through hydrophobic interactions, whereas the bilayer itself is established through strong hydrogen bonding between the zwitterionic amino and acid groups.[1,2] This layered crystal structure is commonly observed in hydrophobic amino acids.[4] The aromatic side chain in L-Phe makes the hydrophobic part exquisitely rich in its ways of stacking compared to other hydrophobic amino acids, which makes it difficult to obtain good quality crystals. Despite the challenges in crystallization, in the past 25 years several crystal structures of L-Phe have been reported, some of which can emerge concomitantly during crystal growth while differing only slightly in the hydrophobic packing of the generic bilayers.[1,5,6]

The electrostatic interactions between neighboring aromatic compounds may translate to so-called edge-to-edge and herringbone structures in the solid-state, often observed in the crystal structure of phenyl-containing compounds. Yet, the aromatic electrostatic interactions in L-Phe and its derivates are subject to a subtle interplay with the zwitterionic hydrophilic part in the crystal structure. Therefore, the terms inter- and intralayer packing are introduced in this work, aiming for a more comprehensive description of these particular aromatic hydrophobic interactions. The interlayer hydrophobic interactions are present between two bilayers, where opposite phenyl groups meet, whereas the intralayer hydrophobic interactions occur between molecules present in the same monolayer. Figure 1a shows the generic bilayered structure, with the inter- and intralayer domains indicated.

In this article, we present the newly obtained crystal structure of *para*-methyl-L-phenylalanine along with the unsubstituted variant L-Phe where we were able to reproduce the literature structure reported by Ihlefeldt et al. (form I).[1] Structure analysis in terms of the inter- and intralayer packing features is shown in Figure 1a. The structural analysis is further expanded to the para-fluorinated variant of L-Phe as reported by In et al.;[8] Figure 1b shows the molecular structures of the compounds investigated. The hydrophobic packing resulting from methyl-substitution turns out to be related to the natural amino acid as well as to its fluorinated variant in a rather surprising way, giving a more comprehensive view on the polymorphism of L-Phe and its derivatives.

EXPERIMENTAL SECTION

Sample Preparation. The growth, selection, and measurement of single crystals was conducted in a similar way for L-Phe and its para-methylated derivative to ensure an unbiased comparison between the two chemically related compounds. D-*para*-Methyl-phenylalanine was purchased from Alfa Aesar, L-*para*-methyl-phenylalanine from AK Scientific, Inc., and L-Phe from Merck. Good quality single crystals of *para*-methyl-L-phenylalanine (Me-L-Phe) and L-Phe were obtained by

Received: May 30, 2017
Revised: September 21, 2017
Published: November 8, 2017

DOI: 10.1021/acs.cgd.7b00747
Cryst. Growth Des. 2017, 17, 6231−6238

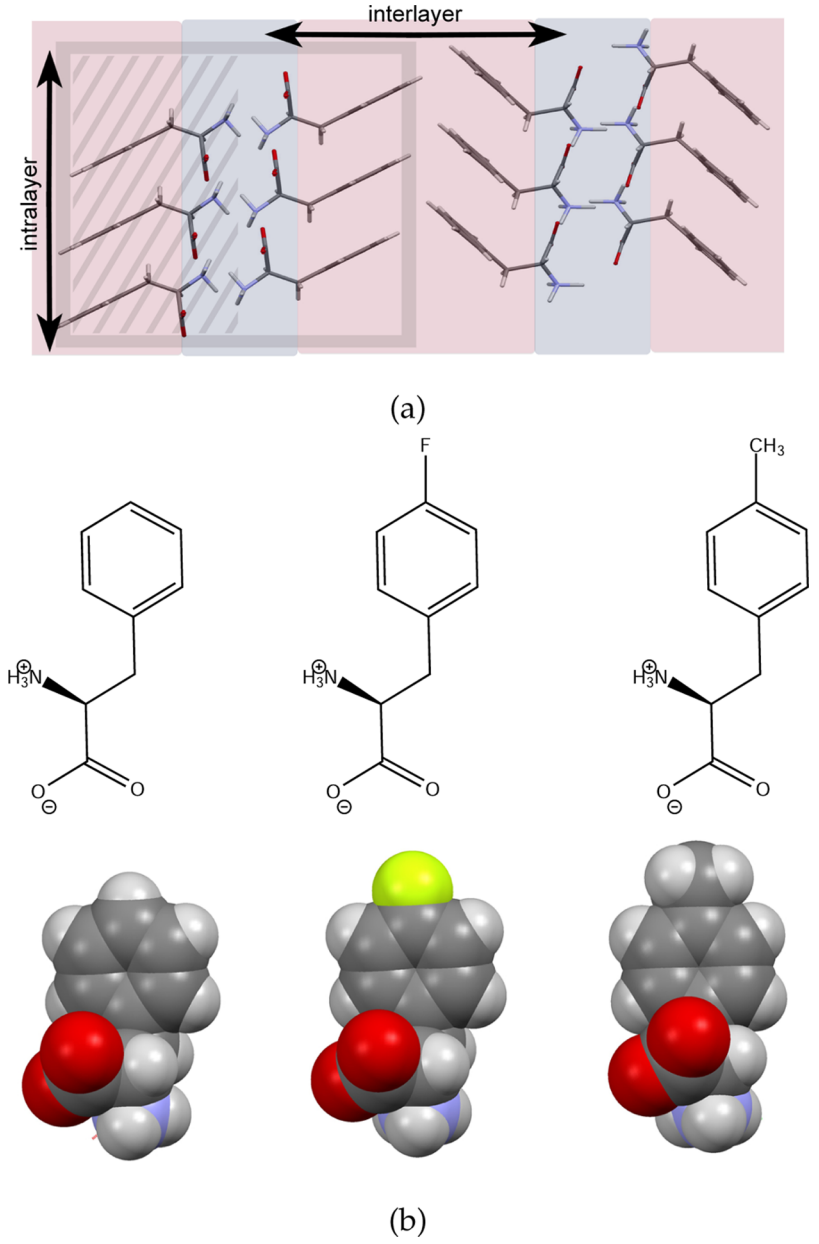

Figure 1. (a) Generic bilayer structure found in amphiphilic phenylalanine and similar compounds. The bilayer and monolayer are illustrated with the crystallographic unit cell of CSD-entry SIMPEJ.[7] Hydrophilic and hydrophobic parts are shown in blue and pink, respectively. A bilayer is indicated by the rectangle, while a monolayer is indicated by the shaded area. The interlayer hydrophobic interactions are present between two bilayers, where opposite phenyls meet, whereas the intralayer hydrophobic interactions are between phenylalanine molecules in the same monolayer. (b) Compounds investigated in this study together with space filling models; molecular structures of L-Phe (left), 4-fluoro-L-phenylalanine (middle), and 4-methyl-L-phenylalanine (right).

vapor diffusion of isopropanol into a nearly saturated solution at room temperature. The compounds were dissolved in water at room temperature up to saturation, and 5 mL of the solution was put in a vial. Before closing the vial with Parafilm, 300 μL of distilled water was added to the solution. Ten small holes in the Parafilm allowed the antisolvent to diffuse slowly into the solution that was placed in a closed Erlenmeyer flask containing the antisolvent isopropanol. Plate-like and needle-like transparent crystals of ~200 μm size were collected after several weeks using filtration through a Büchner funnel. The plate thickness of Me-L-Phe crystals was estimated at 10 μm, whereas L-Phe yielded more block-like crystals with an estimated thickness of 80 μm.

Single-Crystal X-ray Diffraction. The structure determinations for structures A and B were performed on the same crystal at different temperatures.

X-ray Crystal Structure Determination of Structure A. $C_{10}H_{13}NO_2$, F_w = 179.21, colorless needle, 0.54 × 0.08 × 0.04 mm^3, monoclinic, $C2$ (no. 5), a = 43.492(4) Å, b = 6.0810(5) Å, c = 24.705(3) Å, β = 98.090(5)°, V = 6468.7(10) Å^3, Z = 28, D_x = 1.288 g/cm^3, μ = 0.73 mm^{-1}. In total, 10072 reflections were measured on a Bruker Proteum diffractometer with rotating anode and Helios optics (λ = 1.54184 Å) at a temperature of 230(2) K up to a resolution of $(\sin\theta/\lambda)_{max}$ = 0.50 Å^{-1}. The intensities were integrated with the Eval15 software.[9] Multiscan absorption correction and scaling was performed with SADABS[10] (correction range 0.41−0.75). In total, 4982 reflections were unique (R_{int} = 0.053), of which 2862 were observed [$I > 2\sigma(I)$]. The structure was solved using SHELXT.[11] Least-squares refinement was performed with SHELXL 2014[12] against F^2 of all reflections. Non-hydrogen atoms were refined freely with anisotropic displacement parameters. Hydrogen atoms were intro-

DOI: 10.1021/acs.cgd.7b00747
Cryst. Growth Des. 2017, 17, 6231−6238

duced in calculated positions and refined with a riding model. In total, 834 parameters were refined with 631 restraints (concerning displacement parameters). R_1/wR_2 [$I > 2\sigma(I)$]: 0.0831/0.2505. R_1/wR_2 [all refl.]: 0.1209/0.2937. S = 1.043. Partial R-values for the main reflections ($4h + l = 7n$) and the remaining ones ("satellites"): reflections of the subcell, 1663 measured reflections; 735 unique reflections. R_{int} = 0.0486, $\langle I/\sigma \rangle$ = 12.074, $\langle I \rangle/\langle \sigma \rangle$ = 13.185, R_1 = 0.0628 for 714 $F_o > 4\sigma(F_o)$, R_1 = 0.0635 for all 735 data. Reflections of the supercell only (subcell omitted): 8409 measured reflections, 4247 unique reflections. R_{int} = 0.1172, $\langle I/\sigma \rangle$ = 3.543, $\langle I \rangle/\langle \sigma \rangle$ = 5.379, R_1 = 0.1132 for 2148 $F_o > 4\sigma(F_o)$, R_1 = 0.1898 for all 4247 data. Residual electron density between 0.26 and 0.32 $e{\cdot}Å^{-3}$. The absolute structure could not reliably be determined from anomalous dispersion but was assigned according to the known chirality. Geometry calculations and checking for higher symmetry were performed with the PLATON program.[13]

X-ray Crystal Structure Determination of Structure B. $C_{10}H_{13}NO_2$, F_w = 179.21, colorless needle, 0.54 × 0.08 × 0.04 mm^3, monoclinic, $C2$ (no. 5), a = 8.7369(7) Å, b = 6.0529(8) Å, c = 17.3341(11) Å, β = 89.997(8)°, V = 916.69(15) $Å^3$, Z = 4, D_x = 1.299 g/cm^3, μ = 0.74 mm^{-1}. In total, 1827 reflections were measured on a Bruker Proteum diffractometer with rotating anode and Helios optics (λ = 1.54184 Å) at a temperature of 100(2) K up to a resolution of $(\sin \theta/\lambda)_{max}$ = 0.50 $Å^{-1}$. The intensities were integrated with the Eval15 software.[9] Multiscan absorption correction and scaling was performed with SADABS[10] (correction range 0.39−0.75). In total, 726 reflections were unique (R_{int} = 0.042) of which 698 were observed [$I > 2\sigma(I)$]. The structure was solved by direct methods using SIR-2011.[15] Least-squares refinement was performed with SHELXL 2014[12] against F^2 of all reflections. Non-hydrogen atoms were refined freely with anisotropic displacement parameters. Hydrogen atoms were introduced in calculated positions and refined with a riding model. In total, 120 parameters were refined with 127 restraints (distances and angles, flatness of phenyl ring, and displacement parameters). R_1/wR_2 [$I > 2\sigma(I)$]: 0.0653/0.1687. R_1/wR_2 [all refl.]: 0.0674/0.1708. S = 1.072. Residual electron density was between 0.19 and 0.31 $e{\cdot}Å^{-3}$. The absolute structure could not reliably be determined from anomalous dispersion but was assigned according to the known chirality. Geometry calculations and checking for higher symmetry were performed with the PLATON program.[13] Illustrations in Figures 1−8 were created using the CCDC Mercury software.[14]

RESULTS AND DISCUSSION

L-Phenylalanine. A block-shaped transparent single crystal of L-Phe was selected for X-ray diffraction after inspection under a polarization microscope. Block-shaped single crystals were found to grow concomitantly with needle-shaped single crystals. The latter was identified as hydrates using powder X-ray diffraction, in accordance with the literature.[6] These crystals are thought to convert into the anhydrate when kept in solution for longer time, i.e., the needle-shaped hydrate is a metastable form of L-Phe.

The selected block-shaped crystal was shock-frozen from room temperature to 100 K as it was brought into the diffractometer, and a complete data set was collected at this temperature. The structure found is identical to the L-Phe structure, form I in space group $P2_1$, recently reported by Ihlefeldt et al.[1] Therefore, only the unit cell parameters will be presented here. It is noteworthy that Ihlefeldt et al. used vapor diffusion of acetonitrile into a saturated acidic aqueous solution of L-Phe at room temperature. In this study, similar quality crystals were grown via vapor diffusion of isopropanol into a nearly saturated aqueous solution of the pure compound.

L-Phe displays a subtle form of polymorphism, an overview of which is given by Ihlefeldt et al.[1] Single crystals of L-Phe were studied between 100 and 373 K with a rate of 5 K/min using thermal stage polarization microscopy. However, no change in polarization color was observed. Likewise, single-crystal X-ray diffraction measurements with the same temperature gradient did not show a significant change in the diffraction pattern, and we therefore conclude that a solid-state phase transition from form I to any other form of L-Phe does not occur under these conditions.

***para*-Methyl-L-phenylalanine.** *Structure A.* A transparent plate-like single crystal of *para*-methyl-phenylalanine (of the D-enantiomer) was shock-frozen from room temperature to 100 K and measured at 100 K. After structure refinement to an R-value of 5.85%, a commensurately modulated structure with seven molecules in the asymmetric unit was found.

To examine the reproducibility of this crystal structure and for studying a possible solid-state phase transition, a new crystal was grown in a different batch, using new starting material. A transparent needle-like crystal (this time of the L-enantiomer) was shock-frozen from room temperature to 230 K for structure elucidation. The modulated structure (Figure 2a) was found once again, with a final R-value of 8.31% after structure refinement. The well-reproducible structure with Z' = 7 is either the thermodynamically stable crystal structure at higher temperatures or the result of the shock freezing treatment, which causes stress (vide infra). This modulated structure is called structure A. Layered crystals of L-Phe and alike compounds are known to be affected significantly by stress-induced defects. Therefore, special care was taken to mount the crystal as stress-free as possible. Attempts to elucidate the structure at room temperature were not successful because consolidation of the mounting glue probably induced too much stress in the micron-thick plate-like crystal. In this article we only report full structure determinations of structures A and B obtained from the L-enantiomer crystal.

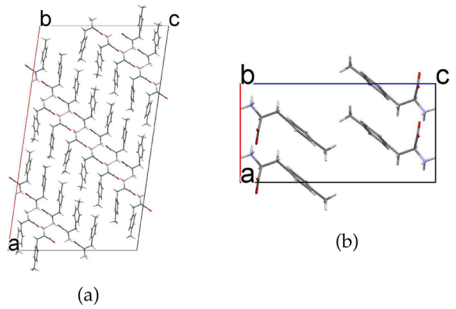

Figure 2. (a) Crystal structure of *para*-methyl-phenylalanine as determined from a single crystal shock-frozen from room temperature to 230 K (structure A). (b) Crystal structure determined at 100 K (structure B) obtained after slowly cooling the same crystal from 230 to 100 K with a rate of 5 K/min. At 100 K, a seven-times smaller unit cell is found. Projections along b.

Structure B. The needle-like crystal of the L-enantiomer, leading to structure A at 230 K, was cooled down to 100 K with a rate of 5 K/min. Surprisingly, at 100 K, a seven times smaller unit cell was found. Figure 2b shows the unit cell of the corresponding crystal structure, refined to an R-value of 6.53%. This structure, having 1 molecule in the asymmetric unit, is called structure B and is the so-called basic structure of A, when the latter is described as a modulated structure. In other words, structure A is a seven-fold superstructure of B, with a modulation along the a-axis of the unit cell of structure B. Structure B shows disorder in the orientation of the phenyl ring (see Figure 3).

DOI: 10.1021/acs.cgd.7b00747
Cryst. Growth Des. 2017, 17, 6231−6238

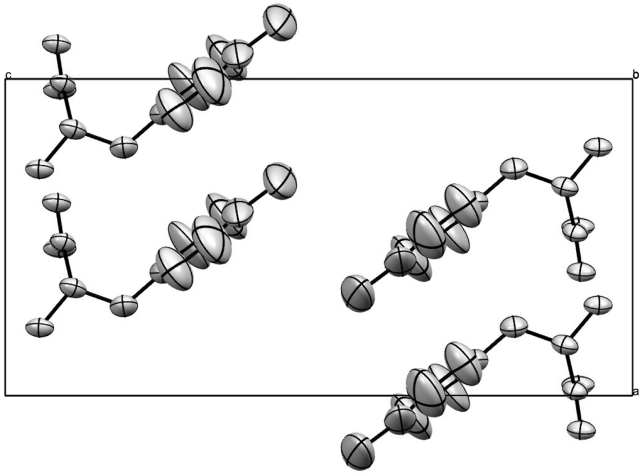

Figure 3. ORTEP drawing of structure B showing the disorder in the phenyl rings.

Comparison of Crystal Structures. *Interlayer Hydrophobic Packing.* As shown in Figure 2, structures A and B are closely related, and a detailed analysis on the differences is therefore necessary. Figure 4a shows a closer view of the structures in Figure 2, illustrating that the interlayer packing, i.e., the interaction between two bilayers, of structures A and B does not change significantly during the phase transition. Judged from Figure 4a, the packing within the bilayer itself is affected due to the seven-fold modulation. This will be addressed further on in the discussion of the intralayer packing features. Figure 4b provides an analogous structure overlay of Me-L-Phe (structure A) and *para*-fluorophenylalanine (F-L-Phe; CSD refcode EXAXEG), which clearly shows that F-L-Phe has the same interlayer hydrophobic packing as Me-L-Phe, recognized as an edge-to-edge like packing of the phenyl rings. Apart from the methyl−methyl distances being larger than the fluorine−fluorine interatomic distances, the overall interlayer packing is unchanged in the case of the *para*-fluorine substituent.

The interlayer packing feature of unsubstituted L-Phe, however, is recognized as a herringbone structure compared to the hydrophobic packing of the para-substituted variants; Figure 5a shows the unit cells of the investigated compounds. Figure 5b,c gives a more detailed view, showing the structure overlay of Me-L-Phe (structure A) with F-L-Phe and L-Phe, respectively, up to three bilayers. From Figure 5 we conclude that the para-fluorinated compound is isostructural with the presently obtained para-methylated compound, except for a

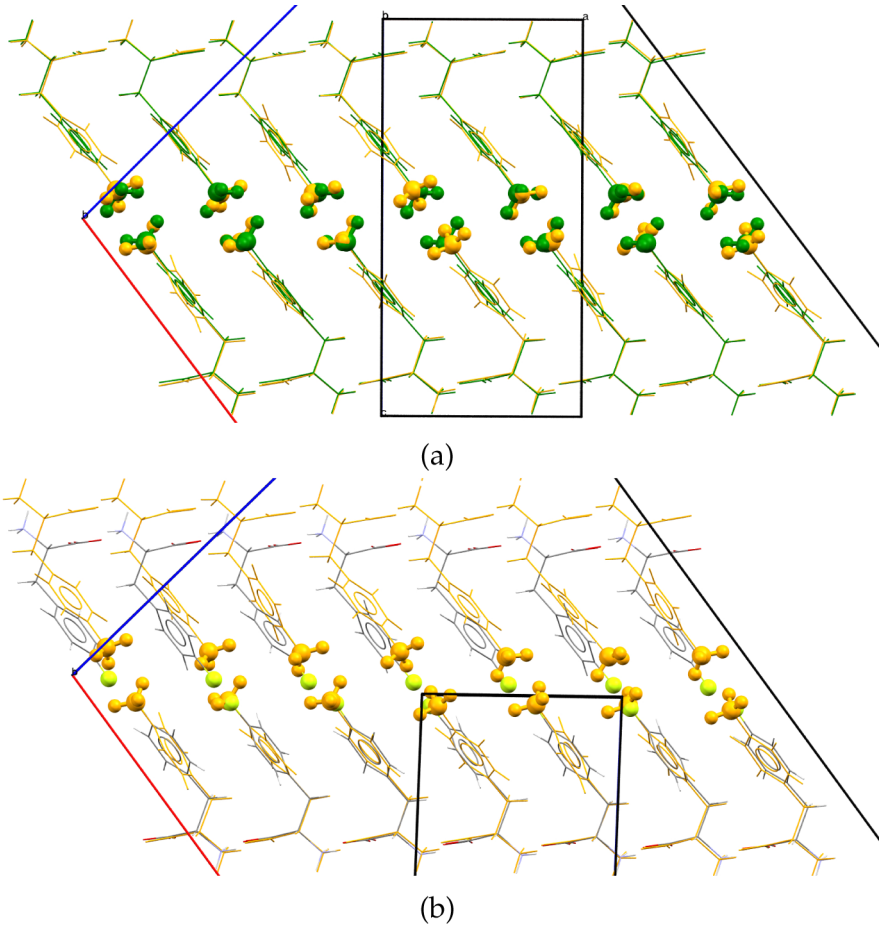

Figure 4. (a) Structure overlay of Me-L-Phe (structure A, yellow) and Me-L-Phe (structure B, green); two complete asymmetric units are shown for illustrating the interlayer packing. The methyl−methyl interatomic distances of structures A and B are similar. (b) Structure overlay of Me-L-Phe (structure A, yellow) and F-L-Phe; the methyl−methyl distances are significantly larger than the fluorine−fluorine interatomic distances. Molecules are represented in wire frame style, while the para substituents are shown in ball-and-stick model for accentuating the interlayer packing. Projections are along *b* of structure A.

DOI: 10.1021/acs.cgd.7b00747
Cryst. Growth Des. 2017, 17, 6231−6238

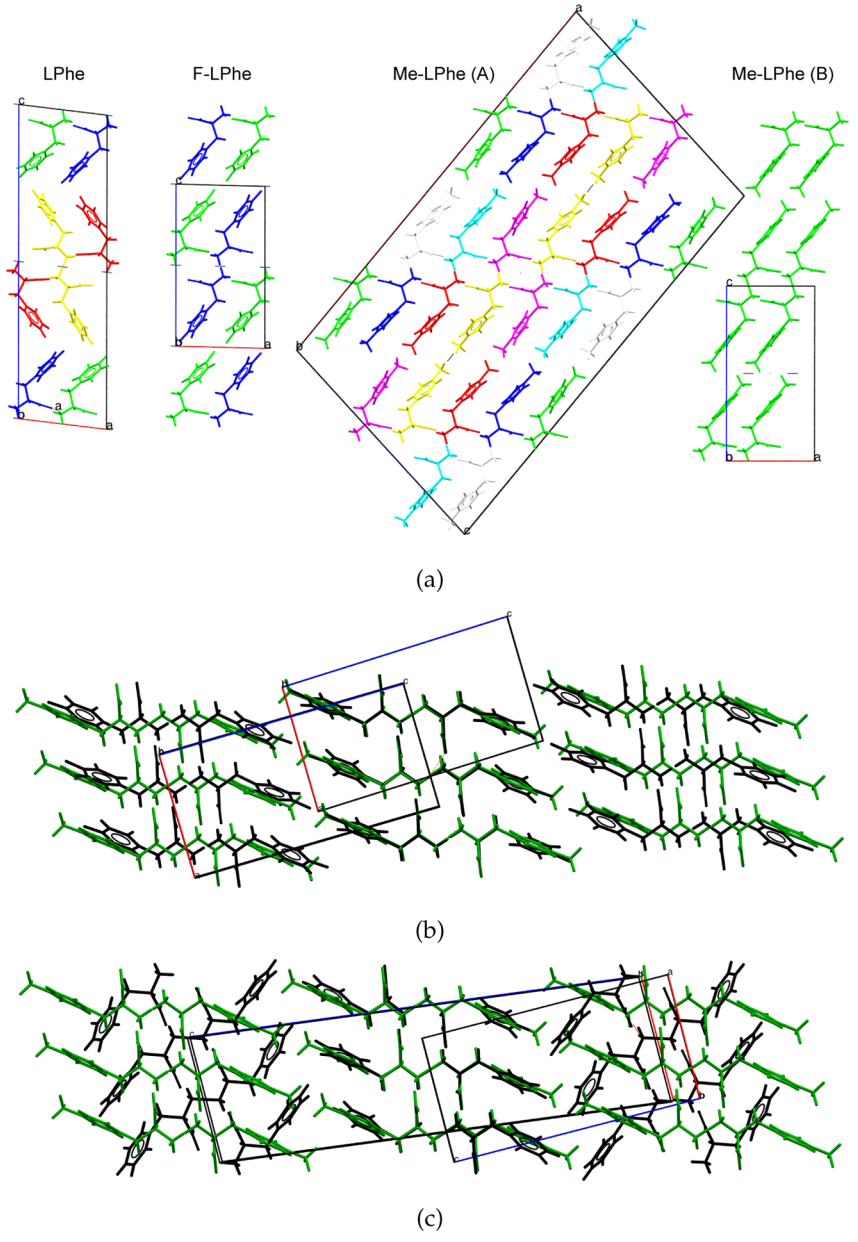

Figure 5. (a) Overview of the unit cells of L-Phe, F-L-Phe, and Me-L-Phe (structures A and B), with projections along *b*. Molecular conformers are colored based on symmetry equivalence. (b) Structure overlay of Me-L-Phe (structure B, green) and F-L-Phe. (c) Structure overlay of Me-L-Phe (structure B, green) and L-Phe. Projections are along *b* of the Me-L-Phe unit cell.

Table 1. Crystallographic Unit Cells of L-Phe and Para-Substituted Derivates

	this work	In et al.[8]	this work (Z' = 7)		this work (Z' = 1)
compd	L-Phe	F-L-Phe	Me-L-Phe	Me-D-Phe	Me-L-Phe
temperature (K)	100		230	100	100
space group	$P2_1$	$P2_1$	$C2$	$C2$	$C2$
a	8.8066(15)	8.8132(10)	43.492(4)	43.385(2)	8.7369(7)
b	6.0049(10)	5.9830(7)	6.0810(5)	6.0701(3)	6.0529(8)
c	31.117(5)	16.0460(18)	24.705(3)	24.6027(13)	17.3341(11)
β	96.844(5)	91.349(2)	98.090(5)	97.728(3)	89.997(8)
volume[a]	816.92	845.86	924.10	917.17	916.89
Z'	4	2	7	7	1

[a]Effective volume for four molecules.

smaller density and a slight difference in phenyl orientation. Table 1 gives structural details for the three related compounds.

It should be noted from Figure 5 that all compounds are perfectly superimposable in the rigid hydrophilic region,

DOI: 10.1021/acs.cgd.7b00747
Cryst. Growth Des. 2017, 17, 6231−6238

meaning that the hydrophilic part retains the same geometry regardless of the hydrophobic part. The hydrogen bonding network in the hydrophilic part is categorized as "hydrogen bond motif III" by Görbitz et al.,[4] and we conclude that the hydrophilic packing of L-Phe remains intact when the compound is para-substituted.

Intralayer Hydrophobic Packing. The phenyl−phenyl geometry within the monolayers, i.e., the intralayer packing, is shown in Figure 6 for Me-L-Phe. The orientation of the phenyl

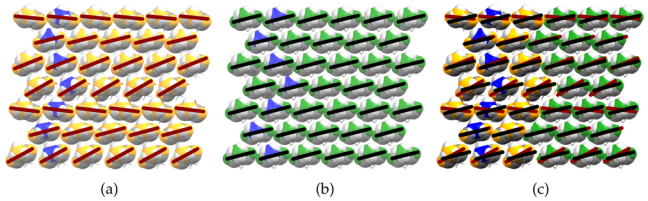

Figure 6. Top view on the hydrophobic layer showing intralayer packing features for (a) structure A and (b) structure B. Phenyl orientations are accentuated by solid lines parallel to the phenyl ring, shown in space-filling representation. For clarity the *para*-methyl substituent and phenyl protons on both sides are shown in yellow for structure A and green for structure B. The methyl substituent of the seven molecules in the asymmetric unit of structure A is colored blue, while the same molecules are colored blue as well in the basic structure B. (c) Overlay of structures A and B with their phenyl orientations accentuated by red and black solid lines, respectively.

ring is indicated by the red and black lines for structures A and B, respectively, showing the subtle change in the intralayer packing going from structure A to structure B.

An extension of the analysis, illustrated in Figure 7, shows that the packing of the monolayer in structure A has common

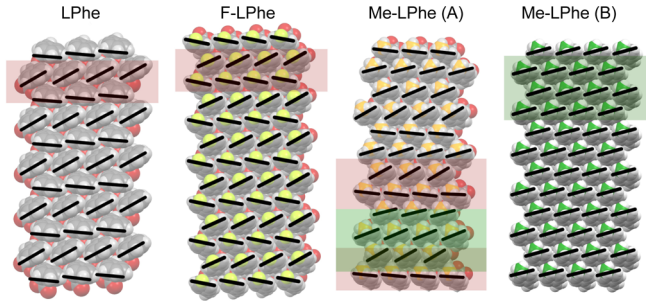

Figure 7. Top view on the hydrophobic side of the monolayer for compounds compiled in Table 1. Phenyl orientations are accentuated by solid lines parallel to the phenyl ring, while the methyl carbon in Me-L-Phe is colored for clarity.

features with both intralayer packings of F-L-Phe and L-Phe: rows of phenyl rings are rotated 45° with respect to each other (indicated with red blocks). In addition, the packing of structure A shows intralayer packing features of the basic structure B as well, with phenyl rings oriented more parallel to each other (indicated with green blocks). Figure 7 clearly shows that Me-L-Phe has a stronger tendency to stack phenyl rings parallel within the same monolayer than L-Phe and F-L-Phe.

The latter observation is intriguing in terms of the interplay between interlayer and intralayer hydrophobic interactions. The steric effect, caused by a specific phenyl substituent in the center of the hydrophobic part (i.e., the interlayer packing), as well as the substituent-specific electron density in the aromatic ring (determining the intralayer packing) accounts for the overall structure and a possible modulation. A particular case of the latter is also found in para- and meta-fluorinated derivatives of L-Phe reported by In et al. where the authors suggest a hydrogen bond-like interaction between fluorine and electron-poor aromatic protons, resulting in specific phenyl geometries in the hydrophobic part of the bilayer. There is no indication for a modulation in the room-temperature crystal structures of para-, meta-, and ortho-fluorinated phenylalanine. All crystal structures obtained after recrystallization at room temperature are unmodulated.[8,16] The modulation in Me-L-Phe might be related to the interplay between the substituent-specific electrostatic aromatic interaction (mainly intralayer) and the substituent-specific steric contribution (mainly interlayer), leading to the observed seven-fold modulation. The absence of relatively strong electrostatic interactions between the hydrophobic layers allows for relaxation of structural stress, possibly induced by the thermal treatment (shock freezing). The disorder in the phenyl ring orientations found in structure B might be due to domain formation upon cooling the sample slowly to 100 K. The domain walls then lead to pinning of the modulation wave and loss of structural coherence.

Modulation and Relation between Structures A and B. To transform the average structure (T = 100 K) into the superstructure (T = 230 K), the following matrix holds (determinant = 7):

$$\begin{pmatrix} a_A \\ b_A \\ c_A \end{pmatrix} = \begin{pmatrix} 3 & 0 & 2 \\ 0 & \bar{1} & 0 \\ 2 & 0 & \bar{1} \end{pmatrix} = \begin{pmatrix} a_B \\ b_B \\ c_B \end{pmatrix} \quad (1)$$

For the back-transformation the inverse matrix can be applied (determinant = 1/7):

$$\begin{pmatrix} a_B \\ b_B \\ c_B \end{pmatrix} = \begin{pmatrix} \frac{1}{7} & 0 & \frac{2}{7} \\ 0 & \bar{1} & 0 \\ \frac{2}{7} & 0 & \frac{\bar{3}}{7} \end{pmatrix} = \begin{pmatrix} a_A \\ b_A \\ c_A \end{pmatrix} \quad (2)$$

The superstructure at 230 K can alternatively be described in (3 + 1) superspace. The cell parameters are then a = 8.7260(8) Å, b = 6.0852(5) Å, c = 17.4252(17) Å, β = 90.202(5)°. The q-vector is (4/7, 0, 1/7), or in decimal notation (0.5716(1), 0.0000(1), 0.1424(3)). The space group is $C2(a0g)0$.

Structure A is a seven-fold superstructure of B. The modulation changes as one moves from one molecule to another along a_B in terms of the basic structure B. This is clearly visible in the structure overlay shown in Figure 8.

The seven independent molecules of the superstructure can be fitted with a quaternion fit.[17] Each molecule is considered independently, and crystal packing effects are ignored. A modulation can be mainly seen in the orientation of the phenyl rings (see Figure 9, Table 2).

Averaging structure A takes the packing effects into account. The structure overlay of the seven independent molecules in structure A then shows that there are slight deviations in the amino acid part of the molecule, but the main modulation remains in the orientation of the phenyl groups as shown in Figure 10.

Apparently, structure A loses its modulation and adapts a higher symmetry with one molecule in the asymmetric unit when slowly cooled from 230 to 100 K. It is remarkable that

DOI: 10.1021/acs.cgd.7b00747
Cryst. Growth Des. 2017, 17, 6231−6238

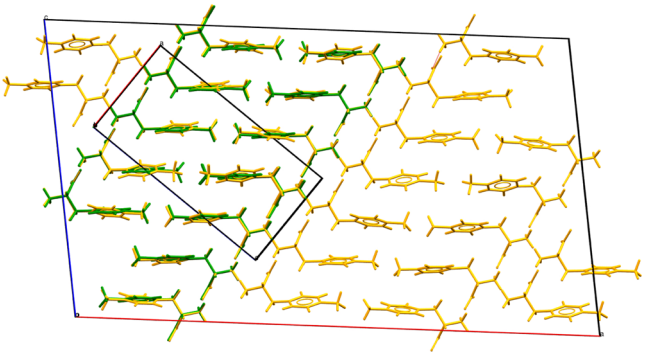

Figure 8. Structure overlay of structures A (yellow) and B (green). Projections along b.

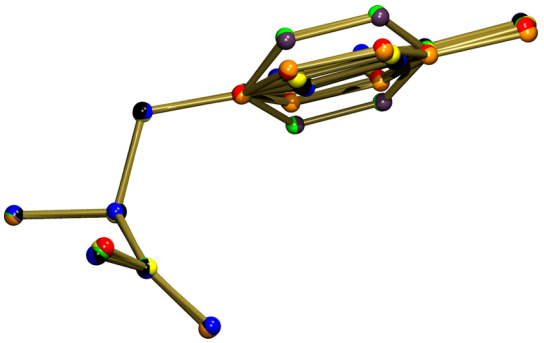

Figure 9. Quaternion fit of the seven independent molecules in structure A. The fit is only based on C1−C4, N, and O atoms. Hydrogen atoms are omitted in the drawing for clarity. The plot was created with the PLATON software.[13]

structure B does not reconvert to structure A upon heating the crystal with the same rate back to 230 K. It must be noted that solid-state phase transitions of amino acids are strongly subject to hysteresis as a result of defects and temperature treatment.[18,19]

The irreversible phase transition has also been studied for Me-L-Phe using thermal stage polarization microscopy for single crystals and using differential scanning calorimetry (DSC) for powders. Single crystals were cooled to 100 K starting from room temperature with a rate of 5 K/min in polarization microscopy. Inhomogeneous color effects were observed, but the temperature at which this was found varied. Therefore, no exact temperature could be identified for the phase transition in these measurements, and we conclude that the subtle phase transition has no significant effect on the optical properties of the crystal. The phase transition was likewise not detectable in DSC measurements on powders. Therefore, the subtle phase transition is only properly observed in single-crystal X-ray diffraction measurements, but akin to phase transitions in comparable amphiphilic systems,[19,20] the study of the solid-state phase transition demands careful and time-consuming repetitions of crystallization and diffraction measurements.

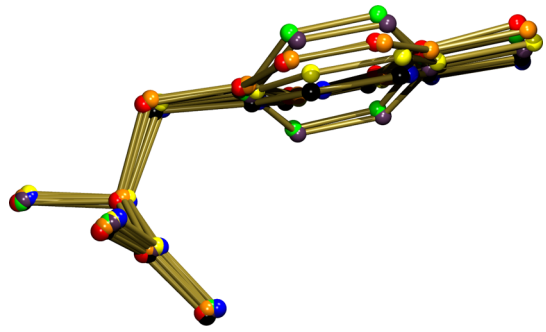

Figure 10. Averaging of the seven independent molecules in structure A according to the transformation matrix (eq 2). Hydrogen atoms are omitted in the drawing.

A final remark should be made on the observed gain of symmetry at 100 K, which is seemingly counterintuitive with the commonly observed loss of symmetry at lower temperatures. For example, *para*-chloro-benzamide (Cl-Bzmd) is a comparable compound becoming three-fold modulated at temperatures below 123 K with respect to the structure at temperatures above 123 K.[21] This compound is reported in literature and is, to the best of our knowledge, the only compound comparable to our amphiphilic bilayered system undergoing structural modulation due to a phenyl substituent.

CONCLUSION

The crystal structure of *para*-methyl-L-phenylalanine at 230 K is a (3 + 1)-commensurately modulated superstructure with seven molecules in the asymmetric unit (structure A), resembling the para-fluorinated variant of L-Phe (EXAXEG) present in the CSD. Structure A loses its modulation at 100 K, leading to a structure B, which is the basic structure of A, with one molecule in the asymmetric unit.

The methyl-substituent in *para*-methyl-L-phenylalanine has, in contrast to fluorine, no polar interaction with protons of neighboring molecules, which may allow for the well-defined modulation of the crystal structure at 230 K. This modulation responds to temperature, as concluded from diffraction measurements. Analysis of intralayer packing features shows that *para*-methyl-L-phenylalanine has a greater tendency to stack parallel within the monolayer, compared to L-Phe and its para-fluorinated variant. The latter is probably the result of both the substituent-specific electrostatic aromatic interaction (mainly intralayer) and the substituent-specific steric contribution (mainly interlayer), leading to the observed seven-fold modulation.

We have shown that a well-defined modulation can be evoked in L-Phe by introducing a methyl substituent on the

Table 2. Torsion Angles in the Seven Independent Molecules in Structure A

molecule	1	2	3	4	5	6	7
C5−C4−C3−C2	56.7(14)	78.1(13)	82.9(13)	94.2(12)	58.3(13)	80.0(12)	90.7(12)
C9−C4−C3−C2	−124.1(12)	−100.8(12)	−94.6(13)	−88.9(13)	−127.5(11)	−98.5(12)	−92.7(13)
C4−C3−C2−C1	67.0(12)	61.5(12)	64.3(13)	68.0(12)	65.8(12)	60.9(13)	71.0(12)
C4−C3−C2−N	−176.2(8)	179.5(9)	−176.0(8)	−171.1(9)	−176.8(8)	179.7(9)	−172.1(8)
C3−C2−C1−O1	−112.9(9)	−113.4(9)	−112.8(9)	−107.8(10)	−112.0(9)	−111.9(10)	−111.5(9)
C3−C2−C1−O2	68.7(10)	68.1(10)	71.8(10)	74.6(10)	69.6(10)	66.7(10)	71.4(10)

DOI: 10.1021/acs.cgd.7b00747
Cryst. Growth Des. 2017, 17, 6231−6238

para position. The observed rich variety of structures for L-Phe and its derivatives, now also including a modulated structure, shows that the phase behavior of this family of compounds, and in particular its dependence on the temperature treatment, offers a challenging field for further research.

■ ASSOCIATED CONTENT

Accession Codes

CCDC 1534132−1534133 contain the supplementary crystallographic data for this paper. These data can be obtained free of charge via www.ccdc.cam.ac.uk/data_request/cif, or by emailing data_request@ccdc.cam.ac.uk, or by contacting The Cambridge Crystallographic Data Centre, 12 Union Road, Cambridge CB2 1EZ, UK; fax: +44 1223 336033.

■ AUTHOR INFORMATION

Corresponding Author

*E-mail: r.degelder@science.ru.nl. Tel: +31 24 3652842. Fax: +31 24 3653067. Web: http://www.ru.nl/ssc.

ORCID

René de Gelder: 0000-0001-6152-640X

Elias Vlieg: 0000-0002-1343-4102

Notes

The authors declare no competing financial interest.

■ REFERENCES

(1) Ihlefeldt, F. S.; Pettersen, F. B.; von Bonin, A.; Zawadzka, M.; Görbitz, C. H. *Angew. Chem., Int. Ed.* **2014**, *53*, 13600−13604.
(2) Mossou, E.; Teixeira, S. C. M.; Mitchell, E. P.; Mason, S. A.; Adler-Abramovich, L.; Gazit, E.; Forsyth, V. T. *Acta Crystallogr., Sect. C: Struct. Chem.* **2014**, *70*, 326−331.
(3) Acharya, A.; Ramanujam, B.; Mitra, A.; Rao, C. P. *ACS Nano* **2010**, *4*, 4061−4073.
(4) Görbitz, C. H.; Vestli, K.; Orlando, R. *Acta Crystallogr., Sect. B: Struct. Sci.* **2009**, *65*, 393−400.
(5) King, M. D.; Blanton, T. N.; Korter, T. M. *Phys. Chem. Chem. Phys.* **2012**, *14*, 1113−1116.
(6) Williams, P. A.; Hughes, C. E.; Buanz, A. B. M.; Gaisford, S.; Harris, K. D. M. *J. Phys. Chem. C* **2013**, *117*, 12136−12145.
(7) Weissbuch, I.; Frolow, F.; Addadi, L.; Lahav, M.; Leiserowitz, L. *J. Am. Chem. Soc.* **1990**, *112*, 7718−7724.
(8) In, Y.; Kishima, S.; Minoura, K.; Nose, T.; Shimohigashi, Y.; Ishida, T. *Chem. Pharm. Bull.* **2003**, *51*, 1258−1263.
(9) Schreurs, A. M. M.; Xian, X.; Kroon-Batenburg, L. M. J. *J. Appl. Crystallogr.* **2010**, *43*, 70−82.
(10) Sheldrick, G. M. *SADABS*; Universität Göttingen: Germany, 2008,.
(11) Sheldrick, G. M. *Acta Crystallogr., Sect. A: Found. Adv.* **2015**, *71*, 3−8.
(12) Sheldrick, G. M. *Acta Crystallogr., Sect. C: Struct. Chem.* **2015**, *71*, 3−8.
(13) Spek, A. L. *Acta Crystallogr., Sect. D: Biol. Crystallogr.* **2009**, *65*, 148−155.
(14) Macrae, C. F.; Bruno, I. J.; Chisholm, J. A.; Edgington, P. R.; McCabe, P.; Pidcock, E.; Rodriguez-Monge, L.; Taylor, R.; van de Streek, J.; Wood, P. A. *J. Appl. Cryst.* **2008**, *41*, 466−470.
(15) Burla, M. C.; Caliandro, R.; Camalli, M.; Carrozzini, B.; Cascarano, G. L.; Giacovazzo, C.; Mallamo, M.; Mazzone, A.; Polidori, G.; Spagna, R. *J. Appl. Crystallogr.* **2012**, *45*, 357−361.
(16) Hiyama, Y.; Silverton, J.; Torchia, D.; gerig, J.; Hammond, S. *J. Am. Chem. Soc.* **1986**, *108*, 2715−2723.
(17) Mackay, A. L. *Acta Crystallogr., Sect. A: Found. Crystallogr.* **1984**, *40*, 165−166.
(18) Perlovich, G.; Hansen, L.; Bauer-Brandl, A. *J. Therm. Anal. Cal.* **2001**, *66*, 699−715.
(19) van den Ende, J. A.; Smets, M. M. H.; de Jong, D. T.; Brugman, S. J. T.; Ensing, B.; Tinnemans, P. T.; Meekes, H.; Cuppen, H. M. *Faraday Discuss.* **2015**, *179*, 421−436.
(20) Görbitz, C. H. *J. Phys. Chem. B* **2011**, *115*, 2447−2453.
(21) Schönleber, P. P. A.; Chapuis, G. *Zeit. Kristall.* **2003**, *218*, 507−513.

DOI: 10.1021/acs.cgd.7b00747
Cryst. Growth Des. 2017, 17, 6231−6238